Inorg. Chem. **2005**, *44*, 4066–4076

Conformational Control of Excited-State Dynamics in Highly Distorted Ru(II) Polypyridyl Complexes

Sherri A. McFarland,[†] Douglas Magde, and Nathaniel S. Finney*[,‡]

Department of Chemistry and Biochemistry, University of California San Diego, 9500 Gilman Drive, La Jolla, California 92093-0358

Received February 21, 2005

Tris(bipyridyl)ruthenium(II) complexes modified such that one of the bipyridines is appended with a crown ether display luminescence that is responsive to complexation with metal ions. The parent species, $Ru(bpy)_3^{2+}$, is moderately luminescent, with an emission lifetime of about 1 μs in fluid solution at room temperature. The modified complexes are much less emissive, with lifetimes near 1 ns. Conformational flexibility and distortion in the crown-ether complexes enhance nonradiative decay. Noncovalent binding of metal ions, however, restores luminescence intensity by reducing nonradiative decay and increasing the lifetime 10- to 100-fold. Reported here are the syntheses and steady-state and time-resolved luminescence measurements in addition to other supporting spectroscopic characterization. Seven metals were investigated; significant luminescence enhancements occur in the presence of Mg^{2+}, Ca^{2+}, and Pb^{2+}. Effective concentrations of metal ions range from tens of μM to hundreds of mM. The steady-state enhancements are readily measured, but they are less than would be expected from the lifetime changes, partly because only a portion (not more than 50%) of the fast (1 ns) decay in $Ru(bpy)_2$(bpy-crown) is capable of converting to the conformation possessing the longer lifetime. A photophysical model is proposed to explain these and other observations.

1. Introduction

Ruthenium polypyridyl complexes exhibit features that are well-suited to chemosensor design: large extinction coefficients, excitation and emission at visible wavelengths, and excited-state lifetimes suitable for biological applications.[1−3] Particularly attractive is a modular design, which allows tuning of ground- and excited-state properties by variation of ligand identity and coordination geometry. Our interest in developing Ru-based sensors was driven in part by our previous work on bi- and polyaryl fluorescent chemosensors that rely on binding-induced conformational restriction as a signaling mechanism.[4,5] While it might initially appear that the bipyridyl ligands in $Ru(bpy)_3^{2+}$ derivatives lack the flexibility needed for such signaling, even small out-of-plane ligand distortions have been shown to have profound effects on both the photophysical and electrochemical properties of these complexes.[6,7]

Steric repulsion between substituents at the 3,3′-positions of a bipyridyl ligand has been shown to produce a species that is much less emissive than the parent $Ru(bpy)_3^{2+}$. This reduced emission has been ascribed, at least in part, to variation in the coordination geometry of the modified bipyridine ligands.[8−11] Such variation affects the energy of the emissive triplet metal-to-ligand charge transfer state, ^{3}MLCT, and its coupling to other states, thereby modulating the luminescence efficiency. The degree of control that can be achieved by this approach has been demonstrated with

* To whom correspondence should be addressed. E-mail: finney@oci.unizh.edu.

[†] Current address: Chemistry Department, Dalhousie University, Halifax, NS B3H 4J3 Canada.

[‡] Current address: Organisch-chemisches Institut, Universität Zürich, Winterthurerstrasse 190, CH-8057 Zürich.

(1) Kalyanasundaram, K. *Photochemistry of Polypyridine and Porphyrin Complexes*; Academic Press: San Diego, 1992.
(2) Juris, A.; Balzani, V.; Barigelletti, F.; Campagna, S.; Belser, P.; Zelewsky, A. V. *Coord. Chem. Rev.* **1988**, *84*, 85.
(3) Kalyanasundaram, K. *Coord. Chem. Rev.* **1982**, *46*, 159.
(4) McFarland, S. A.; Finney, N. S. *J. Am. Chem. Soc.* **2001**, *123*, 1260.
(5) McFarland, S. A.; Finney, N. S. *J. Am. Chem. Soc.* **2002**, *124*, 1178.
(6) Damrauer, N. H.; Cerullo, G.; Yeh, A.; Boussie, T. R.; Shank, C. V.; McCusker, J. K. *Science* **1997**, *275*, 54.
(7) Thummel, R. P.; Lefoulon, F.; Korp, J. D. *Inorg. Chem.* **1987**, *26*, 2370.
(8) Shan, B.; Zhao, Q.; Goswami, N.; Eichhorn, D.; Rillema, D. *Coord. Chem. Rev.* **2000**, *211*, 117.
(9) Perkovic, M. W. *Inorg. Chem.* **2000**, *39*, 4962.
(10) Chiba, M.; Ogawa, K.; Tsuge, K.; Abe, M.; Kim, H.-B.; Sasaki, Y.; Kitamura, N. *Chem. Lett.* **2001**, 692.
(11) Chiba, M.; Kim, H.-B.; Kitamura, N. *Anal. Sci.* **2002**, *18*, 461.

10.1021/ic0502729 CCC: $30.25
Published on Web 05/06/2005

Chart 1. Crown-Ether Bipyridyl Ligands **1**−**3** and Ruthenium Complexes **4**−**6**

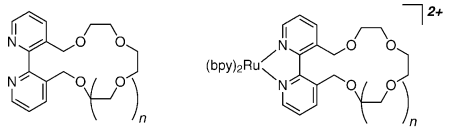

1 n=1
2 n=2
3 n=3

4 n=1
5 n=2
6 n=3

modified bipyridines whose geometry is covalently restricted. In a series of tris-chelated homoleptic complexes containing 2−4 carbon-bridged bipyridines, Thummel et al. demonstrated quantum yields spanning 2 orders of magnitude and emission energies varying by 77 nm (≈1900 cm^{-1}).[7,12] In other complexes containing bipyridine ligands substituted in the 3,3′-positions, steric interactions have also been postulated to cause reduced emission at room temperature.[9−11,13−15] Emission quantum yield is determined by nonradiative processes that occur in competition with radiative decay from ^{3}MLCT states. The two nonradiative processes of primary concern in $Ru(bpy)_3^{2+}$ derivatives are ^{3}MLCT → ^{3}MC internal conversion (IC) and ^{3}MLCT → S_0 intersystem crossing (ISC). Suppression of either channel leads to enhanced quantum efficiencies for luminescence and, in the former case, decreased photochemical decomposition.

In controlling these processes for signaling purposes, it would be preferable that nonradiative decay be maximal in the absence of analyte and minimal in the presence of analyte, such that the sensor would exhibit a low baseline signal until analyte is encountered. It was our hypothesis that these criteria might be met in a system where noncovalent interaction of a modified bipyridine ligand with a guest corrects an inherent distortion in the coordination geometry. To establish proof of principle, we chose to explore ruthenium complexes bearing simple crown-ether-appended bipyridine ligands.[16] For ligands **1**−**3** (Chart 1), the dihedral angles defined by the two rings were expected to vary systematically as the result of steric interactions. Such interactions were anticipated to quench luminescence from the corresponding ruthenium complexes (**4**−**6**) relative to the parent $Ru(bpy)_3^{2+}$ complex. Noncovalent association of the modified bipyridine ligands with external metal ions could then lead to recovery of luminescence, with full planarization restoring $Ru(bpy)_3^{2+}$-like emission.

2. Experimental Section

Synthesis. ^{1}H NMR spectra were obtained on a Varian HG-400 (400 MHz) spectrometer. Chemical shifts (δ) are reported in parts per million (ppm) relative to residual solvent ($CHCl_3$, s, δ 7.26; $(CH_3)_2CO$, m, 2.05). Multiplicities are given as follows: s (singlet), d (doublet), t (triplet), q (quartet), dd (doublet of doublets), or m (multiplet). Proton-decoupled ^{13}C NMR spectra were obtained on an HG-400 (100 MHz) spectrometer. ^{13}C chemical shifts are reported relative to $CDCl_3$(t, δ 77.0) or acetone-d_6(s, δ 29.9, 206.7). Mass spectroscopic analyses were provided by the facility at The Scripps Research Institute (La Jolla, CA) or UCSD Mass Spectrometry Facility (La Jolla, CA). Chromatographic purifications were performed by flash chromatography with silica gel (Selecto, 32−63 μm) packed in glass columns; eluting solvent for each purification was determined by thin-layer chromatography (TLC). Analytical TLC was performed on aluminum plates coated with 0.25-mm sensitized silica gel using UV light. Tetrahydrofuran (THF) was dried by passage through a column of activated alumina. All other reagents and solvents were used as received unless otherwise specified. Ligands **1**−**3** were prepared by minor modification of previously described procedures.[13]

$Ru(bpy)_2(bpy\text{-}O_4)\cdot 2\ PF_6$(4). **1** (0.059 g, 0.18 mmol) and *cis*-dichlorobis(2,2′-bipyridine)ruthenium(II) (0.093 g, 0.18 mmol) were combined in an argon-purged solution of 20% water/ethanol (2.5 mL) under a nitrogen atmosphere and stirred at reflux overnight. Ethanol was removed in vacuo, and saturated potassium hexafluorophosphate was added to the aqueous solution until no further precipitate formed. **4** was collected by vacuum filtration as a brick-red solid (0.147 g, 79%). R_f = 0.41 (20% H_2O/MeCN, 0.5% KNO_3), 0.14 (10% H_2O/MeCN, 0.5% KNO_3); ^{1}H NMR(acetone-d_6), δ: 8.77 (d, 4H, J = 8 Hz), 8.63 (br s, 2H), 8.19 (m, 6H, J = 8 Hz, J = 1.2 Hz), 7.97 (br s, 4H), 7.53−7.38 (m, 6H), 5.22 (br, 2H), 4.49 (br, 2H), 3.9−3.55 (m, 12H); ^{13}C NMR (acetone-d_6), δ: 157.5, 155.3, 152.3, 150.7, 139.5, 138.7, 138.1, 138.1, 127.9, 127.7, 126.5, 124.5, 124.4, 72.3, 70.6, 70.4, 69.8; HRMS (MALDI), *m*/*z*: 743.1993, 567.0547.

$Ru(bpy)_2(bpy\text{-}O_5)\cdot 2\ PF_6$(5). **2** (0.025 g, 0.07 mmol) and *cis*-dichlorobis(2,2′-bipyridine)ruthenium(II) (0.035 g, 0.070 mmol) were combined in an argon-purged solution of 20% water/ethanol (2.5 mL) under a nitrogen atmosphere and stirred at reflux overnight. Ethanol was removed in vacuo, and saturated potassium hexafluorophosphate was added to the aqueous solution until no further precipitate formed. **5** was collected by vacuum filtration as a brick-red solid (0.056 g, 79%). R_f = 0.32 (20% H_2O/MeCN, 0.5% KNO_3); ^{1}H NMR (acetone-d_6), δ: 8.79 (d, 4H, J = 8.4 Hz), 8.63 (br s, 2H), 8.20 (m, 6H, J = 8 Hz, J = 1.2 Hz), 8.00 (br s, 4H), 7.80−7.50 (m, 6H), 4.93 (br, 2H), 4.69 (br, 2H), 3.80−3.40 (m, 16H); ^{13}C NMR (acetone-d_6), δ: 152.9, 151.3, 138.2, 138.1, 138.1, 127.9, 127.7, 124.6, 124.5, 71.5, 70.8, 70.7, 70.2, 69.6; HRMS (MALDI), *m*/*z*: 787.2154, 567.0535.

$Ru(bpy)_2(bpy\text{-}O_6)\cdot 2PF_6$(6). **3** (0.080 g, 0.19 mmol) and *cis*-dichlorobis(2,2′-bipyridine)ruthenium(II) (0.099 g, 0.019 mmol) were combined in a solution of nitrogen-purged 20% H_2O/EtOH (5.0 mL) under a nitrogen atmosphere and stirred at reflux overnight. Ethanol was removed in vacuo, and saturated potassium hexafluorophosphate was added to the aqueous solution until no further precipitate formed. **6** was collected by vacuum filtration as a brick-red solid (0.123 g, 58%). R_f = 0.32 (20% H_2O/MeCN, 0.5% KNO_3); ^{1}H NMR (acetone-d_6), δ: 8.78 (d, 4H, J = 8.0 Hz), 8.60 (br s, 2H), 8.35−8.10 (m, 6H, J = 8 Hz, J = 1.2 Hz), 7.97 (br s, 4H), 7.65−7.35 (m, 6H), 4.87 (br, 2H), 4.73 (br, 2H), 3.70−3.35 (m, 20H); ^{13}C NMR (acetone-d_6), δ: 157.5, 156.0, 152.3, 150.8, 139.8, 138.1, 138.1, 127.9; HRMS (MALDI), *m*/*z*: 831.2469, 567.0557.

Absorption and Emission Spectroscopy. Ruthenium complexes **4**−**6** were synthesized and repeatedly purified via alumina pipet column, eluting with a 0−50% acetonitrile/dichloromethane gradient. Fresh acetonitrile solutions of **4**−**6** (∼1 × 10^{-4} M) were prepared daily and covered with aluminum foil to minimize light-

(12) Strekas, T. C.; Gafney, H. D.; Tysoe, S. A.; Thummel, R. P. *Inorg. Chem.* **1989**, *28*, 2964.
(13) Rebek, J.; Costello, T.; Marshall, R.; Wattley, R.; Gadwood, R.; Onan, K. *J. Am. Chem. Soc.* **1985**, *107*, 7481.
(14) Nakamaru, K. *Bull. Chem. Soc. Jpn.* **1982**, *55*, 2697.
(15) Lai, R. Y.; Chiba, M.; Kitamura, N.; Bard, A. J. *Anal. Chem.* **2002**, *74*, 551.
(16) McFarland, S. A.; Finney, N. S. *Chem. Commun.* **2003**, 388.

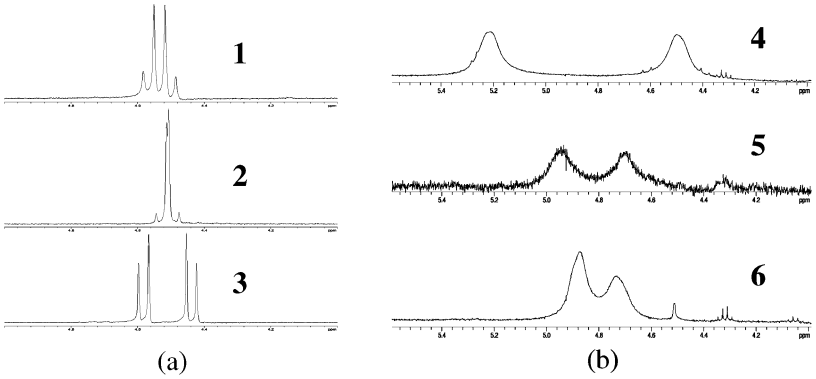

Figure 1. ^{1}H NMR spectra of the diastereotopic methylene protons of **1**−**3** (a) and **4**−**6** (b).

induced decomposition. Dilution in a 1 cm path-length quartz cuvette afforded concentrations on the order of 2.5×10^{-5} M. Steady-state luminescence measurements were carried out in spectroscopic grade CH_3CN on a PTI Quantamaster 2000 with 450 nm flash lamp excitation and 2-nm excitation and emission slit widths. UV−vis absorption measurements were performed on a Cary model 3E spectrophotometer using the same samples employed in the luminescence measurements. Luminescence quantum yields were determined relative to $Ru(bpy)_3^{2+}$, assumed to have a quantum yield of 0.042 in CH_3CN. Measured quantum yields are estimated to be within ±5% of the true values, based on the scatter of repeated measurements. Titrations of **4**−**6** were performed using metal concentrations in the range of 0−100 mM at 23 °C.

Time-Resolved Luminescence Decay. Kinetic analyses were performed on CH_3CN solutions of **4**−**6**. Nanosecond measurements were carried out using the third harmonic of a Nd^{3+}:YAG laser (Quanta Ray DCR2) at 353 nm for excitation at a repetition rate of approximately 1 pulse per second. Luminescence was collected, passed through a glass cutoff filter and a small monochromator (Jobin-Yvon H20), detected by a photomultiplier (Amperex 56TUVP), and digitized by a fast oscilloscope (LeCroy 9361). Most often, decays were monitored at 630 nm. Deconvolution was used to obtain a resolution of about 1 ns. The instrument response function (IRF) was measured at the same wavelength required for samples by using emission from crystal violet in ethanol, a system known to have an excited-state lifetime of no more than a few picoseconds.[17] Temperature-dependent lifetimes were measured for **6** in the absence and presence of 0.04 mM Pb^{2+} and 0.6 mM Ca^{2+}. For variable-temperature measurements, samples were placed in a quartz tube in a cryostat cooled with dry ice/acetone.

More detail of the luminescence decay over the time range 0.05−20 ns was obtained using time-correlated single-photon counting (TCSPC). A frequency-doubled neodymium:vanadate laser with 530-nm output (Coherent Verdi) was used to pump a home-built titanium:sapphire laser that generated femtosecond mode-locked pulses by self-phase-locking. Harmonic doubling of this output provided excitation pulses centered at approximately 400 nm. A portion of the beam was sent to a photodiode to provide "stop" pulses to a discriminator (EGG-Ortec 934). Emission, most often at 630 nm, was sent through a half-meter monochromator (Spex 1870) to a microchannel plate photomultiplier (Hamamatsu 1564U-01). After amplification (Philips 774), the pulses were recognized by a constant-fraction discriminator (Tennelec TC454) to provide "start" signals to the time analyzer (Canberra 2044). The histogram of the delay times between luminescence and excitation was generated by a multichannel pulse-height analyzer (Norland 5300) and transferred to a microcomputer for processing. The IRF to instantaneous emission was measured using a colloidal suspension. Deconvolution was carried out using iterative reconvolution within a least-squares routine based on the Marquardt method.[18]

3. Results

The structures of complexes **4**−**6** were confirmed by standard spectroscopic techniques. Of particular interest were the ^{1}H NMR spectra, which provided important information on the inherent conformational preferences of the complexes in the absence of guest. Steady-state luminescence properties for the complexes were determined as were the properties in the presence of a series of added metal ions potentially capable of interacting with the crown-ether portion of the ligands. In addition, time-resolved emission measurements for **4**−**6** were made, in the absence and presence of added metal ions. In several cases, time-resolved measurements were made at low temperatures in order to better characterize the underlying photophysics involved.

Steady-State Spectroscopic Properties of 4−**6.** The ^{1}H NMR spectra of ligands **1**−**3** indicate that the presence of the 3,3′-substituents substantially hinders bipyridyl rotation at ambient temperature. That these ligands exist as atropisomers at room temperature is indicated by the AB quartets observed for the diastereotopic benzylic methylene protons (Figure 1a). ^{1}H NMRindicates that, while the benzylic methylene protons of **4**−**6** remain diastereotopic, the signals are no longer well-resolved AB quartets (Figure 1b). This apparent loss of resolution will be addressed in the Discussion.

The UV−vis absorption spectrum of a typical heteroleptic ruthenium complex incorporating a crown-ether-appended bipyridine ligand does not differ significantly from that of the parent homoleptic $Ru(bpy)_3^{2+}$ complex, indicating that the incorporation of these ligands does not have a significant impact on the fundamental electronic transitions (Figure 2). Located at approximately 207 nm (48300 cm^{-1}) and 288 nm (34700 cm^{-1}) are ligand-centered $\pi \rightarrow \pi^*$ transitions with extinction coefficients that exceed 3.5×10^4 M^{-1} cm^{-1}. Although transitions located primarily on the metal are Laporte-forbidden and should be weak, there has been speculation that the red-edge shoulder of the LC-centered

(17) Magde, D.; Windsor, M. *Chem. Phys. Lett.* **1974**, *24*, 144.

(18) Marquardt, D. *J. Soc. Industr. Appl. Math.* **1963**, *11*, 431.

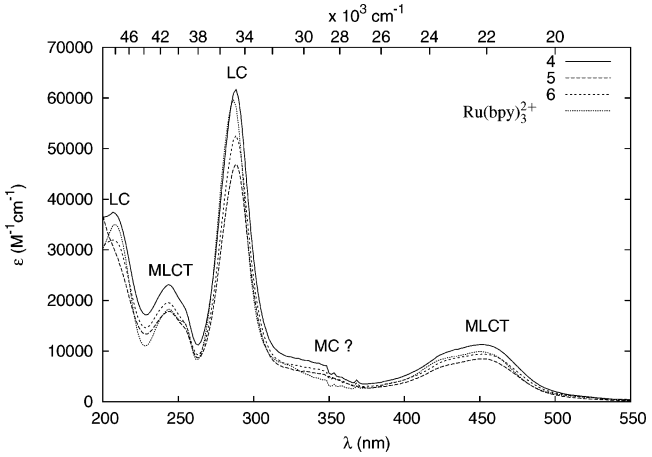

Figure 2. Absorption spectra of **4**−**6** and $Ru(bpy)_3^{2+}$.

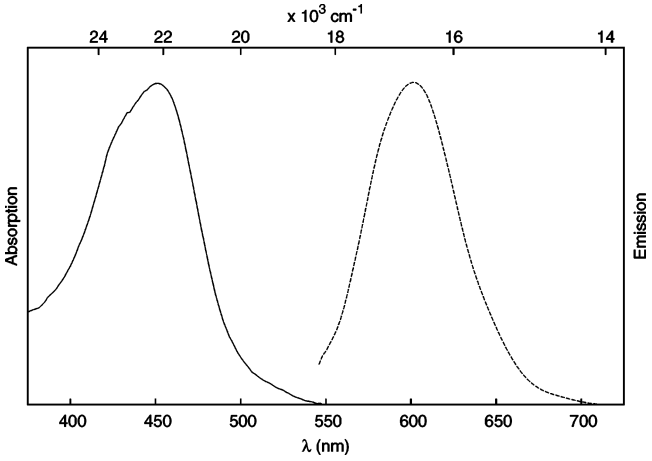

Figure 3. Absorption and emission spectra of **4** (1×10^{-5} M, CH_3CN).

transition at 288 nm may be a $d-d$ transition in $Ru(bpy)_3^{2+}$.[1,2] A similar shoulder, located near 320−375 nm (31300−26700 cm^{-1}) with $\epsilon = 1 \times 10^4$ M^{-1} cm^{-1}, is evident in the spectra of complexes **4**−**6**. MLCT bands occur in both the UV and the visible portion of the spectrum. High-lying ^{1}MLCT transitions occur at 243 and 255 nm (41200, 39200 cm^{-1}) with ϵ slightly less than 2.0×10^4 M^{-1} cm^{-1}. The lowest-lying ^{1}MLCT transitions are centered at 452 nm (22100 cm^{-1}) and at 423−426 nm (23600−23500 cm^{-1}) with ϵ near 1×10^4 M^{-1} cm^{-1}.

Focusing on the emission of **4** as a representative case, excitation into any of the absorption bands leads to emission centered at 600−603 nm (16700−16600 cm^{-1}). This luminescence is most efficient when the excitation wavelength is near 452 nm (22100 cm^{-1}), indicating that a MLCT transition is the emissive state (Figure 3). Because this transition has a large Stokes shift and a long lifetime, it is attributed to a ^{3}MLCT state. These observations are in agreement with those established for the parent $Ru(bpy)_3^{2+}$ system. However, the quantum yields of the modified bipyridine complexes are much smaller than that measured for $Ru(bpy)_3^{2+}$ (Table 1). The low quantum efficiencies throughout the series indicate that the coordination geometry of **4**−**6** is substantially distorted relative to that of $Ru(bpy)_3^{2+}$. As anticipated, this provided for the possibility that "correction" of the distortion in the new complexes upon metal chelation would lead to an increase in the luminescence signal (and possibly a change in the emission wavelength). As described in the next section, titration with a series of metal perchlorate salts demonstrated this to be the case.

Table 1. Photophysical Properties of **4**−**6** in CH_3CN at 298 K

complex	λ_{abs} (nm)[a]	λ_{em} (nm)[b]	ϕ_{air}[c,d]	ϕ_{Ar}[c,d,e]
$Ru(bpy)_2(bpy\text{-}C4)^{2+}$(**4**)	452	601	8.8×10^{-4}	1.5×10^{-3}
$Ru(bpy)_2(bpy\text{-}C5)^{2+}$(**5**)	448	600	1.0×10^{-3}	1.6×10^{-3}
$Ru(bpy)_2(bpy\text{-}C6)^{2+}$(**6**)	452	603	7.0×10^{-4}	1.3×10^{-3}
$Ru(bpy)_3^{2+}$	452	594		4.2×10^{-2}

[a] Absorption maximum of the ^{3}MLCT band. [b] Uncorrected emission maxima at $\lambda_{ex} = 450$ nm. [c] Relative to $Ru(bpy)_3^{2+}$. [d] Experimental ϕ not corrected for contribution from residual $Ru(bpy)_3^{2+}$ (see Results). [e] Samples purged with Ar for 10−15 min prior to measurement.

Steady-State Metal Titrations of 4−6. Solutions of complexes **4**−**6** in CH_3CN were titrated with aliquots of solutions of various metal ions (also in CH_3CN, as perchlorate salts). Observed enhancements in the luminescence emission are reported as I/I_o , where I is the maximum emission intensity reached at a given wavelength, and I_o is the emission intensity at the same wavelength for the complex in the absence of added metal. In selecting an appropriate wavelength for comparing all of the titrations, it is important to note that the complexes do not have identical emission λ_{max} in the absence of metal ions, and the observed λ_{max} may vary as a function of added metal ion. Rather than choose a new comparison wavelength for each titration, in all cases I/I_o was determined at 620 nm (16100 cm^{-1}). This wavelength is very close to λ_{max} for **4**−**6** and is not far from any of the λ_{max} values observed in the titrations. For sensing applications, where it is desirable to maximize I/I_o, it is worth noting that the largest I/I_o values are those measured at the red-edge of the emission.

The steady-state absorption and emission spectra of **4** did not respond significantly to any of the metal ions investigated, so far as could be detected from steady-state luminescence. In titrations of **5** and **6**, Mg^{2+}, Ca^{2+}, and Pb^{2+} gave the largest responses with I/I_o values on the order of ∼3 (Figure 4).[19] The ions Li^+, Na^+, K^+, Cd^{2+}, and Hg^{2+} produced little or no change in either absorption or emission of the complexes studied.

Steady-State Metal Titrations of 5. The metal concentrations at which maximum enhancement occurred in our measurements varies among metals, ranging from 2.6 mM for Pb^{2+} to 230 mM for Mg^{2+}. Complex **5** has a high affinity for Pb^{2+} ion ($K_d \sim 5.3 \times 10^{-3}$ M), as a detectable increase in the luminescence of **5** began to take place at Pb^{2+} concentrations as low as 40 μM, reaching a maximum I/I_o (∼2.1) at approximately 2.64 mM.[19] At higher [Pb^{2+}], I/I_o begins to decrease, presumably reflecting the formation of complexes with >1:1 metal/ligand stoichiometry which differ in their optical properties. Changes in the concentration or

(19) K_d values were determined by nonlinear least-squares fitting of log[metal ion] vs I/I_o (Prism3; GraphPad, Inc., San Diego, CA). In cases where titration with excess metal ion led to eventual reduction of intensity below the maximum I/I_o value, only data up to the point of maximum I/I_o were fit on the basis of the assumption that it is this phase of the titrations that represents the initial formation of 1:1 M/L complex.

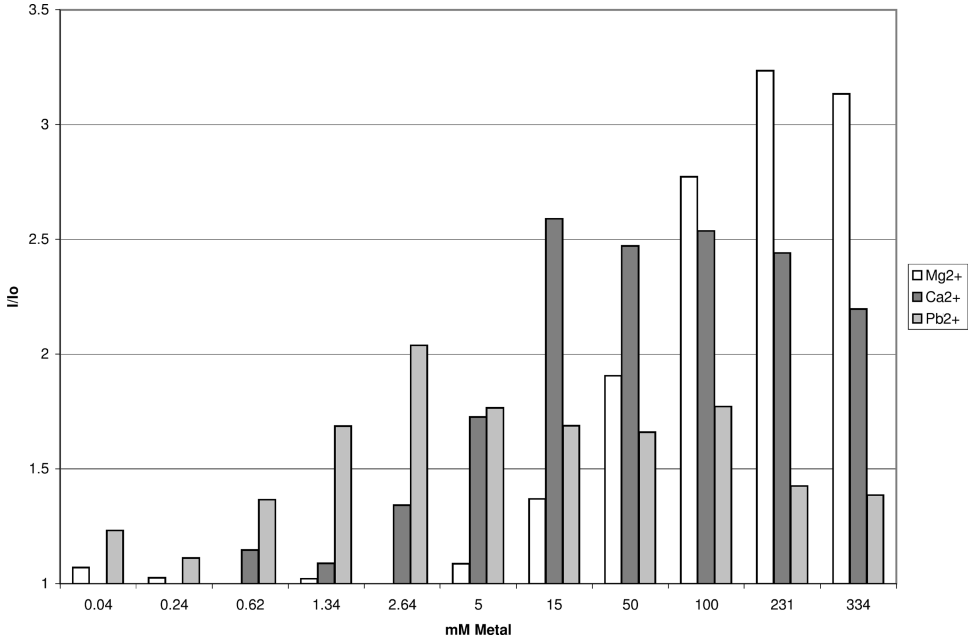

Figure 4. Increased emission from **5** as a function of added metal ions.

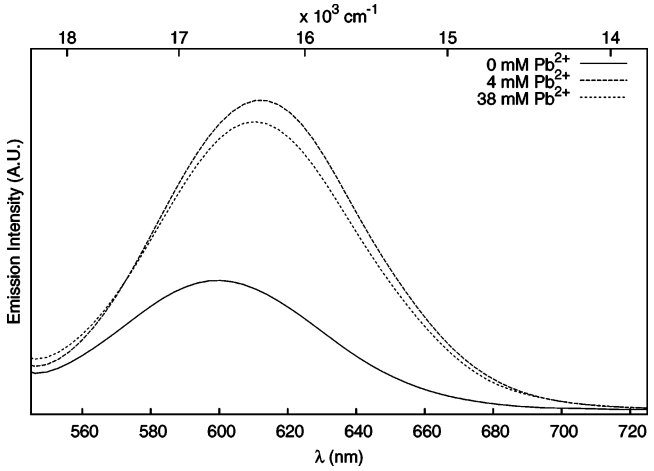

Figure 5. Luminescence titration of **5** with Pb^{2+} ion.

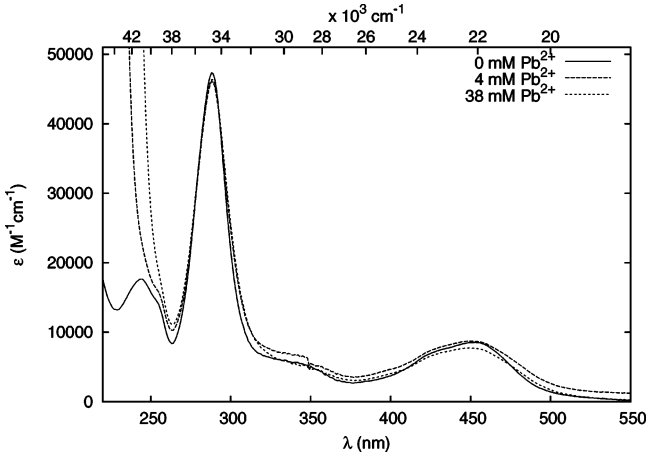

Figure 6. Absorbance response to titration of **5** with Pb^{2+}.

absorption spectrum (Figure 5) are not sufficient to explain the decrease in signal.

Luminescence of **5** began to increase in the presence of Ca^{2+} above 2 mM ($K_d \sim 2.4 \times 10^{-2}$ M). A maximum I/I_o was reached at approximately 15 mM Ca^{2+}, and further addition of metal ion had no effect until dilution began to attenuate the signal. The maximum I/I_o for **5**:Ca^{2+} is approximately 2.6 (Figure 4), and there is a 10 nm ($\sim$270 cm^{-1}) red-shift in the emission maximum for **5** upon Ca^{2+} binding (Supporting Information, Figure S-1). No significant changes occurred in the absorption spectrum of **5** upon titration with Ca^{2+} ion (Supporting Information, Figure S-2).

The largest enhancement of the luminescence efficiency in **5** was produced by high concentrations of Mg^{2+} ion. The onset of emission enhancement began at [Mg^{2+}] $\sim$ 15mM and reached a maximum I/I_o of $\sim$3.2 at 231 mM ($K_d \sim 0.10$ M, Figure S-3). Although this is the largest I/I_o value for the metal ions investigated, the corresponding bathochromic shift (5 nm, 140 cm^{-1}) was much smaller than that observed for **5**:Pb^{2+} or **5**:Ca^{2+}. Thus, at low ion concentrations ($<$5 mM), **5** is capable of signaling almost exclusively Pb^{2+}, while at high concentrations ($>$50 mM), Mg^{2+} elicits the largest response in the series (Figure 4). In the intermediate concentration regime (5 mM $<$ [metal] $\leq$ 50 mM), Ca^{2+} elicits the greatest response.

Steady-State Metal Titrations of 6. The luminescence of **6** also varies as a function of added metal ion with a response profile that is qualitatively similar to that of **5**; the strongest responses were observed on addition of Pb^{2+}, Ca^{2+}, and Mg^{2+} (Figure 7). However, the largest I/I_o values observed in the response of **6** are larger than those for **5**. In addition, there were changes in the binding affinities for the metal ions. The largest enhancement in the luminescence of **6** was triggered by Ca^{2+} ion—as little as 40 μM Ca^{2+} led to an observed I/I_o of $\sim$ 1.5 ($K_d \sim 1.4 \times 10^{-4}$ M, Figure S-4). This ratio increased to a maximum value of $\sim$4.5 at 62 μM Ca^{2+} and diminished thereafter. The hyperchromic effect was accompanied by a bathochromic shift in the emission. The shift from 603 nm (16600 cm^{-1}) to 608 nm (16400 cm^{-1})

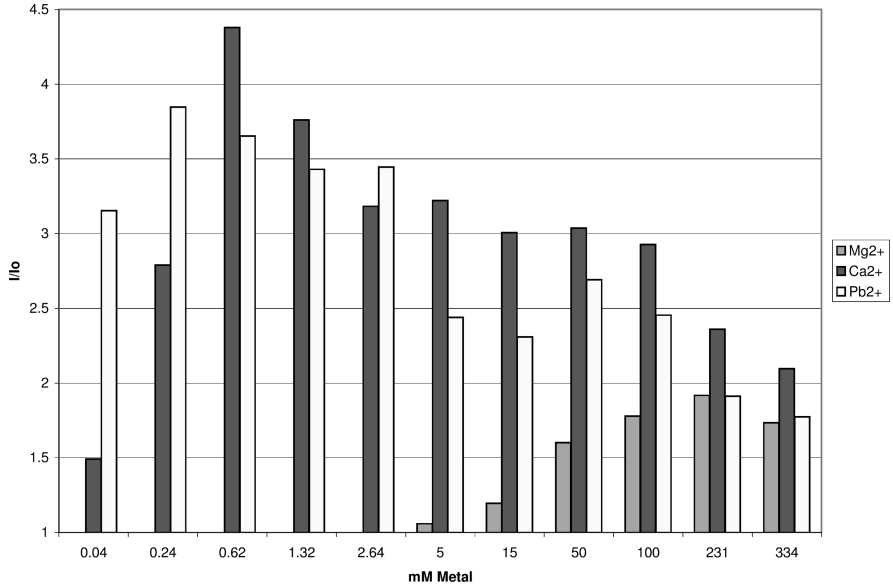

Figure 7. Increased emission from **6** as a function of added metal ions.

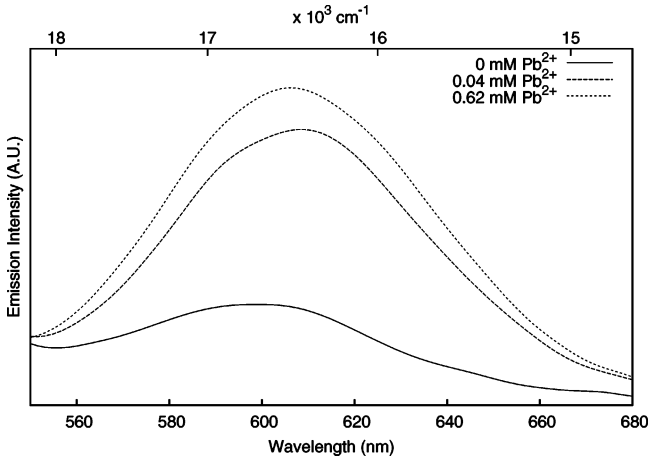

Figure 8. Luminescence titration of **6** with Pb^{2+} ion.

was less than that observed for **5**:Ca^{2+} but was still observable. In the corresponding absorption spectrum of **6**:Ca^{2+}, there were no changes in the positions of the peak maxima, but subtle alterations in the extinction coefficients could be discerned (Figure S-5).

The addition of Pb^{2+} ion to **6** elicited a maximum $I/I_o \sim 3.8$, similar to that for Ca^{2+} but with even greater affinity ($K_d \ll 1 \times 10^{-4}$ M, Figure 8). Below ~40 μM, **6** was almost completely selective for Pb^{2+}. At higher concentrations, the I/I_o began to decrease, as was observed with **5**:Pb^{2+}, again presumably reflecting the formation of higher-order complexes. The increase in I/I_o at 620 nm was accompanied by a bathochromic shift of the same magnitude as that elicited by Ca^{2+} (5 nm, 140 cm^{-1}).

At high concentrations of metal (5−350 mM), **6** responded to Mg^{2+} ($K_d \sim 4.4 \times 10^{-3}$ M). The I/I_o ratio increased over the range of 5−230 mM to a maximum of ~2.1 but decreased again above 230 mM Mg^{2+}. Both Li^+ and Na^+ cause bathochromic shifts in the emission spectrum of **6**, but no corresponding signal enhancements were observed.[20] The luminescence signal was slightly enhanced in the presence of Cd^{2+} and Hg^{2+}, but the enhancements were too small to be of significance.

In summary, complex **4** did not respond appreciably to the presence of added metal ions. In contrast, **5** and **6** responded well to Pb^{2+}, Ca^{2+}, and Mg^{2+}. The relative affinities for Ca^{2+} and Pb^{2+} varied with **5** more readily discriminating between the ions; both complexes exhibited lower affinity for Mg^{2+}. While less selective, **6** responded to ions more strongly (average $I/I_o \sim 4$ for **6** versus ~2.5 for **5**). Subsequent lifetime measurements suggested that the dynamic range of these potential sensors may be larger than the measured I/I_o values indicate, as is discussed in the next section.

Time-Resolved Luminescence of 4−6. Time-resolved measurements distinguish multiple processes that give rise to the luminescence observed in complexes **4**−**6**. In the absence of external metal ions, solutions of **4**−**6** exhibited a biexponential decay at 630 nm with lifetimes of ~1 ns (τ_1) and ~250 ns (τ_2). The luminescence decay could be described as the summation of two processes occurring in parallel (eq 1). The "fast" component (τ_1) had an amplitude (A) more than 100 times that of the "slow" component (τ_2); however, since its lifetime was approximately 1/100 times as long, the two processes made roughly equal contributions to the steady-state luminescence yield (eq 2):

(20) Chiba et al. (references 10 and 11) have published data for **5**:Na^+ which differ from our observations. While we observe only slight steady-state emission enhancements for **5** in the presence of Na^+, Chiba et al. report I/I_o values that exceed 2 at $[Na^+] = 300$ μM. We are unsure of the reason(s) for this inconsistency, as the only apparent experimental difference is their use of deaerated solutions; deoxygenation should increase the contribution of their impurity to the overall steady-state emission, thereby diminishing the maximum attainable I/I_o. There are also notable discrepancies in the time-resolved behavior of **5**:Na^+. Specifically, we observe saturation behavior at or below 50% for all three of our Ru(II) complexes in the presence of various guest ions. Chiba et al. report that 1000-fold excess of Na^+ results in the complete disappearance of the short-lived component ($\tau \sim 4$ ns) with roughly 98% of the emission arising from the longer-lived component ($\tau \sim 22$ ns) when the amplitude and lifetime of the impurity are held constant in the decay analysis.

$$I(t) = A_1 e^{-t/\tau 1} + A_2 e^{-t/\tau 2} \quad (1)$$

$$\int I(t)\, dt = A_1\tau_1 + A_2\tau_2 \quad (2)$$

Time-correlated single-photon counting (TCSPC) measurements indicate that the fast component is a summation of more than one decay, quite possibly a continuous distribution of fast decays, that appears as a single time-averaged process when fitting the nanosecond measurements. The presence of multiple short-lifetime components will be addressed in the Discussion.

The very slow, small-amplitude component had a lifetime of approximately 200−250 ns in the presence of oxygen and slightly less than 1 μs under deoxygenated conditions. The integrated contribution from the slow process was significantly less than 50% for **5**, somewhat greater for **6**, and more than 50% for **4**. The slow component is insensitive to the addition of metal ions and is not thought to be intrinsic to **4**, **5**, or **6** (see Discussion).

Effect of Metal Titration on Luminescence Lifetime. In the presence of metals, the luminescence of **4**−**6** showed a contribution from the fast process (τ_1) which was essentially unchanged in decay time but reduced in amplitude. Upon addition of external metal ions, we observed a new contribution from an intermediate component. The intermediate lifetime (τ_3) varied over ∼10−140 ns, depending on the specific metal complex. The fraction of the initial amplitude associated with the intermediate process increased with metal concentration but saturated at some fraction not greater than 50% (Table 2).[20] As the amplitude of the intermediate component increases, that of the fast component decreases, while the long component remains constant for any given ligand/metal pair. (This is documented in considerable detail in the Supporting Information, Table S1.) The fraction of the initial amplitude that converts to the intermediate component (f_3) was calculated after subtracting the long component (A_2) and is the ratio of the initial amplitude of the intermediate lifetime to the sum of the initial amplitudes for the short and intermediate lifetimes ($f_3 = A_3/(A_1 + A_3)$). The slow component (τ_2) was insensitive to the addition of metal ions. This slow component (with amplitude A_2) was characterized for each solution prior to metal addition so that its contribution could be corrected for in the time-resolved measurements.

For any given metal, the lifetimes associated with complexes of **5** were always longer than those for **6**. Binding of Ca^{2+} and Pb^{2+} saturated at a fraction near or below 50%, and this fraction was lower in **5** than in **6**. Ca^{2+} binding leads to the largest lifetime increases, but Pb^{2+} binds slightly better to **5** and markedly better to **6**. Titrations with Mg^{2+} did not reach a maximum amplitude for the intermediate component over the concentration range studied (≤ 50 mM), consistent with the steady-state observations (vide supra). Notably, the addition of Li^+ and Na^+ led to measurable changes in the lifetime of emission from **5** and **6**, despite the fact that these metal ions induced negligible increases in steady-state emission.

Lifetimes below Ambient Temperature. In an effort to further characterize the photophysical processes unique to the modified crown-ether bipyridine series, the lifetime of **6** was monitored at 23, 0, and −20 °C (Table 3). At 296 K, the decay of **6** was characterized by the short and long components discussed previously. Lowering the temperature to 273 K (0 °C) resulted in the appearance of an additional component with a lifetime of 17 ns, much like the intermediate lifetime observed for the ligand:metal complexes. Further reduction in the temperature to 253 K increased the lifetimes of all components.

4. Discussion

Several aspects of the Results warrant detailed evaluation: (1) the pattern of responses to added metal ion for **4**−**6**; (2) the origin of the short lifetime emission in **4**−**6**; (3) the appearance of the intermediate lifetime (τ_3) in response to added metal ion for **5** and **6** and its saturation point; (4) the persistence of metal ion-independent long lifetime emission; and (5) the origin of enhanced luminescence based on conformational restriction. These will be discussed in order.

Metal Ion Response Profile for 4−**6.** Although complex **4** exhibited essentially no response to added metal ion, complexes **5** and **6** each responded to several metal ions. This was initially surprising, as the biphenyl analogue of **1** binds both Li^+ and Ca^{2+}. The absence of binding observed for **4** most likely results from a combination of the small ring size and the bipyridyl dihedral angle adopted upon complexation of the ligand to Ru(II); the two benzylic oxygen atoms are skewed such that their lone pairs do not point toward any of the other oxygen atoms. This was suggested by simple molecular modeling and confirmed by the recent X-ray structure of a related complex.[21]

Complexes **5** and **6** both respond to the divalent metal ions Ca^{2+}, Mg^{2+}, and Pb^{2+}. This is not particularly surprising; the free crown-ether bipyridyls **2** and **3** are known to bind metal ions, as are the biphenyl analogues of **1**−**3**. Furthermore, the vast crown-ether literature suggests that virtually all crown ethers may be expected to bind at least one, and often numerous, metal ions. However, the details of these binding events—the specificity and affinity of a crown for a given metal ion—are extremely difficult to predict since the "size-fit" model quickly breaks down as structures depart from the parent crown ethers (for example, 18-crown-6). As has been discussed, this reflects the importance of numerous effects other than ionic radius (such as lone-pair orientation, solvation, counterion, and transannular interactions).[22,23] It is presumably the interplay of variables such as these that determine the observed ion-response profile for **5** and **6**. In addition, as will be discussed, the mechanism by which ion-binding-induced conformational restriction enhances the luminescence of biphenyl crown ethers (suppression of

(21) Dutta, S.; Gan, D.; Perkovic, M. *Eur. J. Inorg. Chem* **2003**, 2812−2819.
(22) Martell, A.; Hancock, R.; Motekaitis, R. *Coord. Chem. Rev.* **1994**, *133*, 39.
(23) Hancock, R. *Analyst* **1997**, *122*, R51.

Table 2. Representative Time-Resolved Luminescence Titrations of **4**−**6** with Various Metal Ions

complex	**4**	**5**	**5**	**5**	**6**	**6**	**6**	**5**	**5**	**6**	**6**
M^{n+}	Pb^{2+}	Pb^{2+}	Ca^{2+}	Mg^{2+}	Pb^{2+}	Ca^{2+}	Mg^{2+}	Li^{+}	Na^{+}	Li^{+}	Na^{+}
$[M^{n+}]$ (mM)	50	5	50	50	0.05	5	50	50	50	50	50
τ_3 (ns)	33	71	135	108	43	61	55	27	23	8	11
f_3	0.01	0.31	0.23	0.11	0.42	0.31	0.16	0.34	0.39	0.16	0.29

Table 3. Temperature Dependence of Time-Resolved Emission from **6**

T (K)	A_1	τ_1 (ns)	A_3	τ_3 (ns)	A_2	τ_2 (ns)
296	0.99	2.0			0.01	195
273	0.82	1.7	0.16	17	0.01	225
253	0.85	4.0	0.14	60	0.01	265

intersystem crossing) is completely different from the mechanism by which conformational restriction in **4**−**6** appears to operate.

Analysis of the Short (τ_1)-, Intermediate (τ_3)-, and Long (τ_2)-Lifetime Emissions. The behavior observed for luminescence decay is consistent with metal ions binding to the crown-ether cavity of **4**−**6**, suppressing nonradiative decay and giving rise to a new, longer-lifetime emissive state. An increasing amplitude of a new component, as observed here, is expected for a simple titration of binding sites by a reagent (that is, metal ions). These observations and interpretation differ from other reports in which a single lifetime was said to lengthen steadily in proportion to the amount of metal present.[10,11] We have not yet been able to account for this discrepancy, although we note that it requires quite good data over a range of conditions before the introduction of additional fitting parameters is justified. In addition, there is reason to believe that relatively small changes in temperature near ambient could mask the presence of the intermediate lifetime state (vide infra). In the absence of clear-cut data on other complexes, it would have been quite difficult to analyze the behavior of **4**−**6** toward the alkali metals.

(1) Origin of the Short-Lifetime Emission (τ_1). $Ru(bpy)_3^{2+}$ exhibits moderate luminescence ($\phi \sim 0.042$) from the lowest ^{3}MLCT excited state in acetonitrile solution at room temperature. The phosphorescence decays with an exponential lifetime of 1.04 ± 0.05 μs in our measurements and is reduced to 200 ±10 ns in air-saturated solutions. Tethering the 3,3′-positions of one of the bipyridyl ligands through a crown-ether linkage to form complexes **4**−**6** results in more than a 100-fold decrease in the luminescence and a change in the decay kinetics to a superposition of lifetimes (the average of which is τ_1, as described in the previous section) near 1 ns in duration and independent of the presence of oxygen.

We ascribe the appearance of the fast-lifetime (τ_1) emission to a distortion in the coordination geometry of the 3,3′-substituted bipyridyl (relative to uncoordinated 2,2′-bipyridine). For a rigid, planar bidentate ligand, nonradiative decay is at a minimum when the bite angle of the chelating heteroatoms is 90° and the dihedral angle defined by the planes of the two pyridine rings is 0°. Deviations in either angle may lead to a lowering of the ^{3}MC state and/or an increase in the number of active vibrational modes coupling the ground and ^{3}MLCT states, both of which would reduce

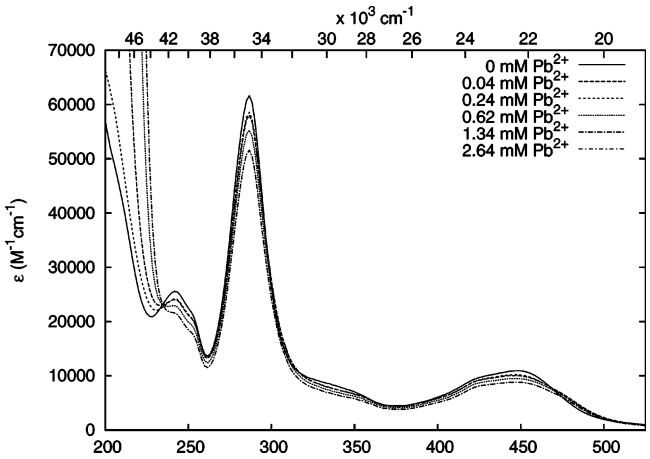

Figure 9. UV−vis absorption titration of **6** with Pb^{2+} ion.

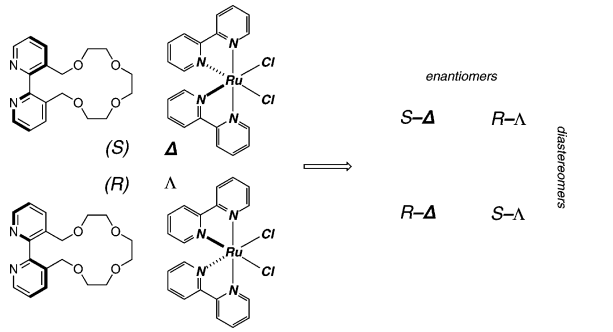

Figure 10. Formation of diastereomeric Ru(II) complexes, illustrated for **4**.

the excited-state emissive lifetimes.[7,12,24] Recent X-ray crystallographic studies on **5** and **6** show substantial deviation from planarity with **5** exhibiting a 35° dihedral angle for the crown-appended bipyridyl and **6** exhibiting a 25° dihedral angle.[21]

The postulate that τ_1 is, in fact, the sum of more than one lifetime is consistent with the existence of **4**−**6** as mixtures of diastereomers. As noted in the Results, ^{1}H NMRsignals for the benzylic methylene protons of **1**−**3** appear as well-resolved AB quartets. This indicates that the benzylic protons are diastereotopic and that the bipyridyl ligands exist as enantiomers (atropisomers) that do not readily interconvert at room temperature. The chirality of these ligands has significant consequences for the formation of complexes **4**−**6**. Since the $[Ru(bpy)_2Cl_2]^{2+}(PF_6^-)_2$ precursor exists as a mixture of Δ and Λ isomers and **1**−**3** exist as enantiomers, complexes **4**−**6** must be formed as mixtures of the four possible diastereomers (Figure 10).[25] Consistent with this, ^{1}H NMR spectra of **4**−**6** indicate that, while the benzylic

(24) Henderson, L. J.; Fronczek, F. R.; Cherry, W. R. *J. Am. Chem. Soc.* **1984**, *106*, 5876.
(25) Zelewsky, A. V. *Stereochemistry of Coordination Compounds*; John Wiley and Sons: West Sussex, 1996.

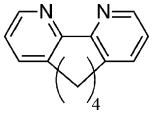

Figure 11. daf-4.

methylene protons remain diastereotopic, the signals are no longer well-resolved AB quartets (Figure 1). This loss of resolution indicates that the signals are superimposed signals for the two pairs of racemic diastereomers. For clarity in the following discussions, we will refer to the diastereomers formed from the Δ and Λ Ru(II) precursors and the S and R bipyridyl crown-ether atropisomers as S-Δ, S-Λ, R-Δ, and R-Λ.

Complexes **4**−**6** are thus formed as mixtures of diastereomers. While these mixtures are racemic, it is not necessarily the case that there are equal populations of the diastereomers. Thummel et. al. determined that one enantiomeric pair of $Ru(bpy)_2(daf\text{-}4)^{2+}$ (Figure 11) isomers is thermodynamically more stable than its diastereomeric counterpart.[7,26] Molecular modeling has shown that significant steric interaction between H_6 and $H_{6'}$ is avoided when coordination occurs in the form of R-Δ and S-Λ. This reasoning can be extended to **4**−**6**. If the diastereomers **4**−**6** are not equal in energy, it is likely that solutions used are unequal mixtures of diastereomers. This, in turn, provides a simple interpretation for the observation of more than one short lifetime emission; the nonequivalent diastereomers **4**−**6** each exhibit short (<1 ns) but nonequivalent lifetimes. In addition, on the sub-nanosecond time scale, individual conformations of each diastereomer could exhibit similar (but not identical) lifetimes, allowing for the observation of >2 lifetimes for a single pair of diastereomers.

While we cannot accurately determine the distribution of processes summed as τ_1 (the short lifetimes approach instrumental resolution), a strong case for emission from two diastereomers (and conformers thereof) can be made on the basis of the above discussion and observations made regarding the intermediate lifetime emission (τ_3).

(2) Origin of the Intermediate Lifetime Emission (τ_3) and Its Saturation Behavior. Upon addition of Ca^{2+}, Mg^{2+}, or Pb^{2+} to solutions of **5** or **6**, the intensity of luminescence emission increases. Time-resolved measurements reveal that the contribution to emission from the short-lifetime (τ_1)-state(s) decreases, and a new emissive state appears with an intermediate lifetime (τ_3). The increase in steady-state emission intensity (I/I_o) is proportional to the fractional contribution of this intermediate emission (f_3) as a function of added metal ion, and both values reach their maxima at the same metal ion concentration (Table 4). (Note that the lifetime data for **5**:Mg^{2+} were acquired at well below the saturating [Mg^{2+}], and these data have been omitted from the table.) While there is not a clear relationship between I/I_o and f_3 or K_d, it is interesting to note that f_3 and K_d themselves can be correlated for each ligand. This, in turn, suggests that more favorable binding events are better able to overcome the entropic cost of conformational restriction and thus more strongly influence the emissive lifetime, although this is admittedly speculative.

Table 4. Correlation of Steady State and Lifetime Titration Measurements

complex	**5**	**5**	**6**	**6**	**6**
metal ion	Pb^{2+}	Ca^{2+}	Pb^{2+}	Ca^{2+}	Mg^{2+}
I/I_o(max)	2.1	2.6	3.7	3.5	1.9
f_3	0.31	0.23	0.42	0.31	0.16
K_d (M)	5.3×10^{-3}	2.4×10^{-2}	1×10^{-4}	1.4×10^{-4}	4.4×10^{-3}

It is also worth noting that the time-resolved data from titrations of **5** and **6** with Li^+ and Na^+ (Table 2) provide a clear indication that metal ion binding is not a sufficient condition for increased luminescence emission: the maximum f_3 for each of these titrations reflects a significant population of crown ether/metal ion complex; however, these binding events lead to only small (albeit measurable) changes in τ_3, and thus to only small increases in I/I_o. This stands in marked contrast to observations on the corresponding biphenyl crown-ether systems, where complete correlation of metal ion complexation and increased fluorescence emission are observed.[4,5]

Even after the metal response has reached saturation, the fractional contribution of the intermediate state (τ_3) does not exceed 50% of the initial amplitudes of the fitting function. It is important to note that the contribution of τ_3 to the total steady-state emission is the product $A_3\tau_3$; therefore, the fraction of the steady-state luminescence due to τ_3 can be much greater than 50%. The observation that not all of the short component can be converted to the new, intermediate component with increasing metal concentration suggests that there are at least two subpopulations of complexes **5** or **6**, one of which responds to the addition of metal ion while another does not.

A simple explanation for this behavior also arises from the stereochemistry of complexes **4**−**6**. Each complex exists as a mixture of diastereomers. In the absence of metal ions, emission from both diastereomers is fast (<1 ns). The observed changes are well-explained by the following scenario: one diastereomer is incapable of binding metal ions as a result of the bipyridyl crown ether being forced into a conformation that is too rigid or too distorted to allow metal−crown complexation while the other diastereomer, with a different conformation, is capable of binding metal ions in a way that alters the overall conformation of the transition-metal complex. This change in conformation, in turn, increases both the lifetime and the emission efficiency, leading to the appearance of the intermediate lifetime state.

This model is also supported by the low-temperature, time-resolved emission studies of **6**. In the absence of metal ion, the room-temperature emission from **6** is adequately described by the short lifetime (τ_1) and the long lifetime (τ_2). As the temperature is lowered, the intermediate lifetime (τ_3) appears which is synonymous with what is seen for metal ion binding. Thus, lowering the temperature has the same effect as adding a metal ion. Again, this is most easily understood by assuming that one diastereomer of **6** is rigid and, therefore, relatively insensitive to temperature effects while the other diastereomer is more flexible. This more

(26) Wu, F.; Thummel, R. P. *Inorg. Chim. Acta* **2002**, *327*, 26.

flexible diastereomer exhibits reduced conformational freedom when metals are bound or the temperature is lowered, leading to an increased lifetime. It should be pointed out that reduced flexibility does not a priori ensure the appearance of the intermediate component. Rather, we hypothesize that it is the reduced flexibility of the crown cavity in conjunction with a more favorable geometry for the overall transition-metal complex that leads to longer lifetime emission.

There are two additional implications of the observation that one of the two diastereomers exhibits temperature-dependent emission near room temperature. First, it provides an explanation for the fact that the intermediate lifetime emission has not been previously observed: at temperatures slightly above ambient temperature, thermal-activated decay of the "flexible" diastereomer could easily predominate. Second, since these observations indicate that the "rigid" diastereomer is not conformationally flexible at ambient temperature, it raises the possibility of studying the rigid diastereomer at higher temperatures where dynamic processes would be more important. Under such conditions, it might be possible to study the emission from the rigid diastereomer without interference from the flexible diastereomer, if thermal-activated decay does become important.

(3) Persistent Slow (τ_2) Emission. A persistent impurity with a long luminescence lifetime produced a background contribution that diminished I/I_o to a factor less than 5. Since the trace contaminant has a longer lifetime than the metal-induced luminescence, deoxygenation serves to reduce I/I_o values; therefore, our results are reported for air-saturated solutions. The contaminant, present at levels well below 1% relative to the complexes, might be $Ru(bpy)_3^{2+}$; traces of $Ru(bpy)_3^{2+}$ have plagued others,[9] and repeated purification is required. A sample of pure $Ru(bpy)_3^{2+}$ in acetonitrile gave a single lifetime near 200 ns in aerated solution and 1.04 μs in the absence of oxygen at 23 °C which is not unlike the lifetimes measured for the impurity. Mass spectrometry showed a small peak possibly consistent with the presence of $Ru(bpy)_3^{2+}$ with an amplitude considerably less than 1% of the parent peak. However, there are arguments against the long component being simply and exclusively $Ru(bpy)_3^{2+}$; the synthesis was designed to minimize such contamination, multiple purifications were performed, the measured lifetimes are slightly different, and, most importantly, the amount of impurity increases over a period of days. This increase is accompanied by a new peak in the absorption spectrum at ~420 nm (23800 cm^{-1}) which is inconsistent with the ^{1}MLCT maximum for $Ru(bpy)_3^{2+}$ (452 nm).

Influence of Conformational Restriction on Emission. The notion that one of the diastereomers is rigid and insensitive to metals while the other is flexible and metal-responsive was introduced above. Because the lifetime of the short component does not exhibit a significant temperature dependence, as would be expected for an activated process, and because the luminescence is extremely short-lived, we believe that vibronic coupling between the ^{3}MLCT state and the ground state ensures an efficient mode of nonradiative decay for some conformations. In contrast, the temperature dependence of the intermediate component and its appearance in conjunction with metal ion binding suggest that an activated process is more important in preventing luminescence under ambient conditions for the intermediate component (which is presumably a different conformation).

The observation that decay profiles for the fast processes are heterogeneous at all temperatures is not surprising since the crown cavities in complexes **4**−**6** involve rings of 16−22 atoms. Even for a fairly rigid conformer, there are likely to be slight conformational variations centered around some geometry possessing a potential energy minimum, resulting in a distribution of lifetimes. As long as there is some mobility, the shorter-lived conformations will be sampled, and the net effect will be fast decay.

Two principle distortions are known to increase the efficiency of nonradiative decay via different means. For a rigid, planar bidentate ligand, nonradiative decay is at a minimum when the bite angle of the chelating heteroatoms is 90° and the dihedral angle defined by the planes of the two pyridine rings is 0°. Deviations in either angle may lead to a lowering of the ^{3}MC state and/or an increase in the number of active vibrational modes coupling the ground and ^{3}MLCT states. Previous work[7,12,24] suggests that the temperature-dependent population of the LF state is governed by in-plane distortions while temperature-independent nonradiative decay to the ground state is facilitated by out-of-plane distortions. Because ligand exchange takes place from the excited ^{3}MC state, the slow decomposition of complexes **4**−**6** in acetonitrile solution shows that the LF state is accessible at room temperature. Furthermore, there is literature precedent for enlarged dihedral angles when the 3,3′-positions in bipyridine are bridged by three or more atoms.[7] Therefore, we expected that the modified bipyridine ligands in **4**−**6** would exhibit both in-plane and out-of-plane distortions, as confirmed by recent X-ray crystallographic data,[21] and that both temperature-dependent and temperature-independent modes of nonradiative decay are important.

5. Conclusion

The results of this work show that the efficiency of Ru(II) luminescence can be modulated via ion-binding-induced conformational restriction of bipyridyl ligands. Luminescence signaling in these systems is feasible because nonradiative partitioning between excited-state manifolds is subject to conformational constraints. In particular, the conformation of the crown-ether ring determines the amount of distortion that takes place at the chelating site of the bidentate ligand, which affects the degree of orbital overlap between the metal and ligand. If enough conformational flexibility is present in the complex, then the extent of σ-bonding between ligands and metal can be used as a switch whose position is controlled by the presence or absence of metal in the crown cavity. In the absence of metal, luminescence is effectively turned "off", and maximal distortion ensures that the e_g orbitals are sufficiently low in energy that nonradiative decay through this channel predominates. The binding of external metal ions provides the "on" trigger which corrects the

distortion, leading to effective σ-bonding between the ligand and metal. An increase in the ligand field strength of the coordinating ligand results in the destabilization of the metal e_g orbitals and virtually no change in the ligand π^* energy as confirmed by electrochemical potentials measured for **5**.[15] Experiments to establish the mechanism responsible for metal ion signaling in compounds **4**−**6** are ongoing, and it should be possible to obtain definitive answers by integrating further variable-temperature luminescence decay experiments with NMR and electrochemical methods. Information gleaned from such measurements will not only provide interesting insights from a basic photophysical perspective, but also will direct the focus for the next generation of sensors based on conformational restriction in ruthenium complexes containing modified bipyridine ligands. For practical applications, selectivity must be increased by replacing the generic crown-ether domain with a more analyte-specific moiety, and the decomposition reaction must be eliminated. The search for practical solutions to these problems will undoubtedly lead to interesting insights and possibly further our current understanding of ruthenium polypyridyl photophysics.

Acknowledgment. The authors thank the National Science Foundation for support of this research (CHE-9876333) and the Departmental NMR Facilities (CHE-9709183). D.M. thanks the late Prof. K. Wilson.

Supporting Information Available: Additional steady-state and time-resolved spectroscopic data (pdf). This material is available free of charge via the Internet at http://pubs.acs.org.

IC0502729